Structured combustion catalysts based on sintered metal fibre filters

I. Yuranov, L. Kiwi-Minsker[*], A. Renken

Institute of Chemical Engineering, LGRC-EPFL, CH-1015 Lausanne, Switzerland

Abstract

Novel efficient structured combustion catalysts based on sintered metal fibre filters (MFF) were developed. To increase specific surface area (SSA), metal fibres were coated by crack-free porous oxide films of SiO_2, Al_2O_3, porous glass, and mesoporous SBA-15 silica. The composite materials presented uniform open macrostructure of the non-treated MFF filters and were suitable supports for deposition of catalytically active phases (Pd, Pt, and Co_3O_4). These catalysts were tested in hydrocarbon (CH_4, C_3H_8) combustion. Co_3O_4 supported on MFF without any coating (6.8% Co_3O_4/MFF) was the most active for propane total oxidation. At the same time in methane combustion the activity of this catalyst was relatively low. Pd supported on the MFF coated by mesoporous SBA-15 film (0.5% Pd/SBA-15/MFF) demonstrated the highest activity in methane total oxidation due to the high palladium dispersion.

The SBA-15 film supported on MFF provided the highest dispersion of the deposited noble metals (Pd, Pt) with an average particle size ~2.0 nm. The metal nanoparticles formed within the mesopore channels were stable against sintering during calcination and the particle diameter was observed not to exceed the diameter of the silica pores. These catalysts did not undergo deactivation under reaction conditions at temperatures up to 500 °C. On the contrary, the Pd supported on MFF coated by the microporous SiO_2 and Al_2O_3 films, prepared by sol–gel technique, suffered from metal sintering during the calcination step and also during reaction, demonstrating strong catalyst deactivation.

The catalytic filters are suitable materials for assembling different multiple layers to obtain structured catalytic beds with the composition/concentration gradients of active component in the axial direction. The enhanced overall catalytic performance was observed in adiabatic catalytic reactor during propane combustion due to a synergy of the 0.5% Pd/SBA-15/MFF and the 0.5% Pt/SBA-15/MFF catalytic layers assembled in the appropriate order forming gradient catalytic bed.
© 2002 Elsevier Science B.V. All rights reserved.

Keywords: Combustion catalysts; Metal fibre filters; Oxide film coating; Pd, Pt/SBA-15 film; Gradient structured catalytic bed

1. Introduction

The choice technology for the treatment of automobile exhausts and various industrial emissions is catalytic combustion. In catalytic reactor-incinerators the requirements of low pressure drop lead to the replacement of random packing by a regular catalyst arrangement, which is also known as "structured catalyst". Commercially available structured combustion catalysts are usually ceramic or metallic monoliths with open channels. They have well-known advantages compared to randomly packed catalytic beds [1]. Noble metals or transition metal oxides supported on the oxide outer layer (washcoat) of monoliths are

* Corresponding author. Tel.: +41-21-693-31-82;
fax: +41-21-693-31-90.
E-mail address: lioubov.kiwi-minsker@epfl.ch (L. Kiwi-Minsker).

effective catalysts for total oxidation of volatile organic compounds. Recently, we have shown that the catalysts based on woven glass fibres [2,3] and metal wire grids [4–6] are suitable for the design of structured combustion reactors. Glass fibre materials made from very thin filaments ($d = 5$–$20\,\mu m$) have open regular macrostructure providing a low pressure drop during the gas passage in addition to mechanical elasticity and thermal shock resistance. Catalytic beds arranged from metal wires ($d = 50$–$500\,\mu m$) present an open regular structure and suitable mechanical properties. Due to their high thermal conductivity, a decrease in the hot spots formation is observed in exothermic reactions. The creation of a porous oxide layer on the metal surface is necessary for active phase deposition.

Sintered metal fibre filters (MFF), consisting of thin metal filaments ($d = 2$–$30\,\mu m$) [7] combine the advantages of structured metal wires with the properties of fibrous materials. The micro-fibrous metal filters are mechanically and chemically stable. Available in the form of panels of different thickness, they possess uniform highly porous 3D macrostructures with porosity ranging between 70 and 90%. High thermal conductivity of the metal fibre matrix provides a radial heat transfer coefficient in the catalytic bed about two times higher compared to randomly packed beds [8], resulting in nearly isothermal conditions in the reactor. The micro-fibre matrix acts also as a micron scale static mixer avoiding channelling. The small fibre diameter allows to obtain a thin oxide coating increasing specific surface area of the MFF. At the same time thin coating renders the catalyst with improved mass transfer resistance since the pores are short and the reactant diffusion does not limit the reaction. Another advantage of the catalytic filters is the simultaneous filtration of solid particles and combustion of gaseous pollutants.

The goal of this study was to develop efficient combustion structured catalysts based on sintered MFF and to test them in the total oxidation of propane and methane. The materials are suitable for assembling catalytic layers with different composition to built structured adiabatic combustion reactors. The MFFs, made of temperature stable alloy (Inconel 601), were coated by a uniform porous oxide layer in order to increase the MFF specific surface area and to stabilise the supported active component against agglomeration. Palladium, platinum and cobalt oxide as

catalytically active phases were investigated. In order to establish a relationship between catalyst activity and active phase dispersion depending on the surface morphology and chemical composition of the support, different types of oxides, like SiO_2, Al_2O_3, porous glass and mesoporous SBA-15 silica were deposited on the MMF.

2. Experimental

2.1. Materials

Sintered metal fibre filters Bekipor ST 20AL3 (Inconel 601) in the form of a panel with thickness of 0.49 mm was supplied by Bekaert Fibre Technology (Belgium) and used as a support for the catalyst preparation. This material consisting of thin metal fibres ($d = 6$–$12\,\mu m$) has porosity of 81% and wetness capacity of $\sim 40\,wt.\%$.

LUDOX AS-40 colloidal silica (Aldrich, 40 wt.%) and poly(ethylene glycol)-poly(propylene glycol)-poly(ethylene glycol) block copolymer, $EO_{20}PO_{70}$-EO_{20} (Aldrich: Pluronic 123, $M_{av} = 5800$) were used to prepare SiO_2 and SBA-15 films. All other chemicals ("purum") were supplied by Fluka.

2.2. Catalyst preparation

Different oxide films deposited on metal fibres are listed in Table 1.

The sol–gel solvent evaporation method [10,11] was employed for the synthesis of silica, alumina and mesoporous SBA-15 films. A Vycor-type porous glass layer was prepared *via* deposition of the precursors of sodium borosilicate glass components on

Table 1
Catalytic supports based on sintered metal fibre filter (MFF)

Support	Coating preparation method	Oxide content (wt.%)	SSA (m²/g)	Pore size (nm)
MFF	–	–	<1	–
SiO₂/MFF	Sol–gel	5.0	19	<2
Al₂O₃/MFF	Sol–gel	5.0	13	<2
SBA-15/MFF	Sol–gel	5.5	40	6.0
PG/MFF	Glass film preparation + acid treatment	4.5	16	<2

the fibre surface followed by their melting and acid treatment [12–14]. As it is known, the melt of sodium borosilicate glass, when cooled below its liquidus temperature, separates into two intertwined phases: a phase soluble in strong mineral acids and an insoluble one. Acid treatment of the phase-separated glass removes the soluble phase resulting in a porous ($d = 1$–5 nm) silica-enriched glass.

In a typical SiO_2 coating preparation, 5 ml of H_2O and 5 ml of concentrated HCl were added into the solution of 20 g of tetraethoxysilane (TEOS) in 30 ml of ethanol with stirring for 2 h at 70 °C. The MFF were impregnated with this solution, dried at room temperature for 14 h, and calcined in air at 450 °C (2 h). The SiO_2 content was determined gravimetrically to be 5.0 wt.%.

The Al_2O_3 coating was prepared as reported in [15] using the solution containing 17.5 g of $Al(i\text{-}C_3H_7O)_3$ with 8.6 g of acetylacetone in 50 ml of ethanol. The solution was cooled down and 50 ml of ethanol containing 3.1 ml of H_2O were added slowly under vigorous stirring resulting in a sol at pH 4.5. The MFF were impregnated with the final solution, dried at room temperature (14 h). The impregnation and drying were repeated. The filters were calcined in air at 450 °C for 2 h resulting in Al_2O_3 content of 5.0 wt.%.

The solution for the mesoporous SBA-15 film coating was prepared as described elsewhere [16,17]. An ethanol solution of Pluronic 123 was mixed at room temperature with a silica gel solution prepared from TEOS, ethanol, water and HCl by stirring for 2 h at 70 °C. The molar ratio of the components in the final solution was TEOS:Pluronic 123:H_2O:HCl:ethanol = 1:0.016:4.4:0.04:11. After impregnation with this so-

lution, the porous metal fibre filters were dried at room temperature for 14 h, calcined in air at 500 °C for 3 h resulting in SBA-15 content of 5.5 wt.%.

In the Vycor-type porous glass (PG) coating preparation, the precursors of the sodium borosilicate glass components were deposited onto the MFF filters *via* impregnation. Two solutions of the precursors were used for this purpose: (a) a mixture of 10 ml of colloidal silica (40 wt.%) and 90 ml of H_2O and (b) a solution of $Na_2B_4O_7 \cdot 10H_2O$ (12.3 g) and $B(OH)_3$ (3.65 g) in H_2O(100 ml). The MMF were impregnated with the first solution and dried at room temperature for 14 h and subsequently at 100 °C for 2 h. The impregnation and drying operations were repeated using the second solution. The MMF were heated in air at 800 °C for 2 h to create glass (7 wt.% Na_2O + 23 wt.% B_2O_3 + 70 wt.% SiO_2) film on the metal fibre surface with a content of 7.5 wt.%. The glass film was treated in HCl (3 wt.%) at 80 °C for 1 h, rinsed and dried in air at room temperature.

The catalysts based on the coated metal fibre supports were prepared by impregnation with Pd-$(CH_3COO)_2$, $Pt(NH_3)_4Cl_2$ and $Co(NO_3)_2$ aqueous ammonia solutions of desired concentrations followed by drying at room temperature and calcination in air at 450 °C for 1 h. For the purpose of comparison some catalysts were prepared by impregnation of non-coated MFF with the $Pd(CH_3COO)_2$ and $Co(NO_3)_2$ aqueous ammonia solutions. The main parameters of all synthesised catalysts are listed in Table 2.

2.3. Catalyst characterisation

The Pd and metal oxide loadings were measured gravimetrically and by atomic absorption spectroscopy

Table 2
Catalysts based on the coated metal fibre filters (MFF)

Catalyst	SSA_{cat} (m^2/g)	SSA_{coat} (m^2/g)	Pore size (nm)	$d_{Pd(Pt)}$ (nm)	Pd[a] dispersion (%)	$T_{50\%(C_3H_8)}$ (°C)	$T_{50\%(CH_4)}$ (°C)
0.5% Pd/MFF				70.0	1.6		445 (deact.)
0.5% Pd/SiO_2/MFF	17	350	<2	44.1	2.5	370	~500 (deact.)
0.5% Pd/Al_2O_3/MFF	12	240	<2	33.6	3.3	365	410 (deact.)
0.5% Pd/SBA-15/MFF	38	710	5.7	1.7	66.0	290	325
0.5% Pd/PG/MFF	16	350	<2	3.9	29.8	300	335
0.5% Pt/SBA-15/MFF	38	710	5.7	2.0	–	240	~500 (deact.)
6.8% Co_3O_4/MFF				–	–	235	435 (deact.)
1.4% Co_3O_4/SBA-15/MFF	24	440	3.9	–	–	395	–

[a] Measured after methane combustion.

using a Shimadzu AA-6650 with an air–acetylene flame.

The specific surface area (SSA) of the supports and catalysts were measured using N_2 adsorption–desorption at $-196\,^{\circ}C$ by a Sorptomatic 1990 (Carlo Erba) instrument. The catalysts were heated in vacuum at $250\,^{\circ}C$ for 2 h prior to the surface area measurements. The SSA of the samples was calculated employing the BET method while the Dollimore/Heal method was applied for the calculation of pore volume and pore size distribution (PSD).

The dispersion of Pd and Pt was determined by CO pulse adsorption (3 vol.% CO in He) at $50\,^{\circ}C$ *via* a Micromeritics 2910. The samples were pre-treated in a flow of H_2 at $300\,^{\circ}C$ during 1 h and subsequently in He flow at $300\,^{\circ}C$ during 1 h. A Pd surface density of 1.2×10^{19} atoms m^{-2} and a stoichiometry factor $SF_{Pd} = CO/Pd$ of 0.6 were used for the SSA_{Pd} calculations.

X-ray diffraction (XRD) spectra were performed on a D500 Siemens powder diffractometer (Cu $K\alpha_1$) in the angle range of 0.5–10° 2Θ with the steps of 0.02° and a step time of 8 s.

The surface morphology of the synthesised supports and catalysts was investigated *via* scanning electronic microscopy (JSM 6300F, JEOL).

2.4. Measurement of catalytic activity in total oxidation of hydrocarbons

The catalytic activity measurements were carried out in a stainless steel continuous flow fixed-bed reactor (Fig. 1). The structured catalytic bed was arranged as three filters (~ 0.8 g), with the diameter equal to the inner diameter of the reactor, placed into the middle section of a big tube and fixed by two short tubes of a smaller diameter. The reactor was sealed by Teflon rings. Gas mixtures of C_3H_8 (0.5 vol.%) or CH_4 (1 vol.%) and oxygen (10 vol.%) in argon was used for the catalytic tests. The propane, methane, oxygen and argon provided by Carbagas (Lausanne, Switzerland, >99.99%) were used as received without any further purification. The flows of gases were controlled by mass flow controllers. A gas flow of 100 ml min^{-1} (STP) was used throughout the study. During the catalytic testing the reactor was heated up and afterwards cooled down stepwise waiting for stabilisation (1 h) at each step. The reaction temperature was monitored by a thermocouple placed in contact with the catalytic
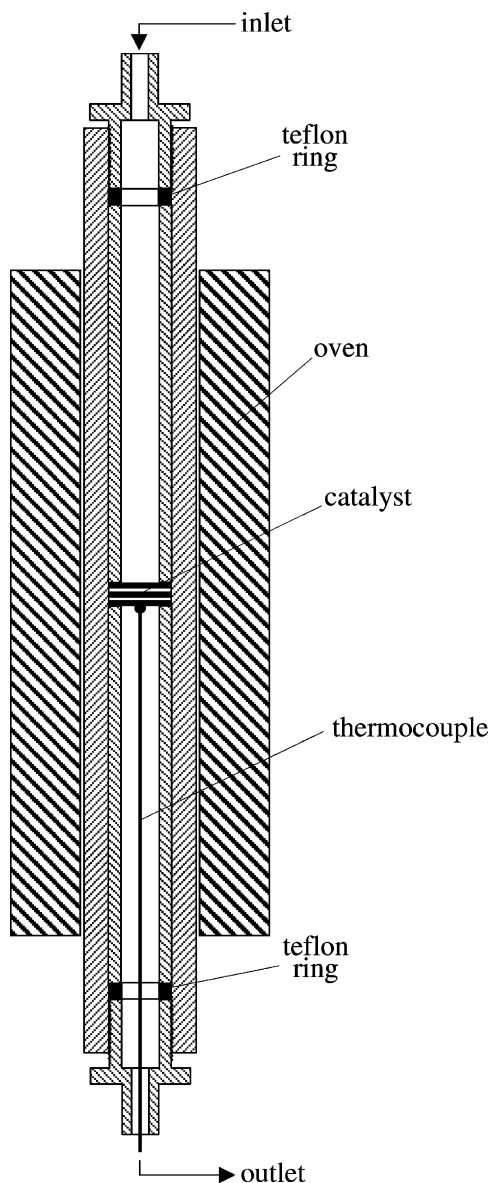

Fig. 1. Scheme of the reactor with a multilayered structured catalytic bed for hydrocarbon total oxidation.

filters. Only CO_2 and H_2O were found as the products of the C_3H_8 and CH_4 oxidation over the catalysts used in this study. The outlet concentration of CO_2 was continuously monitored by an infrared analyser Ultramat 22P (Siemens). The temperature necessary for the hydrocarbon conversion of 50% was used to compare the catalyst activities.
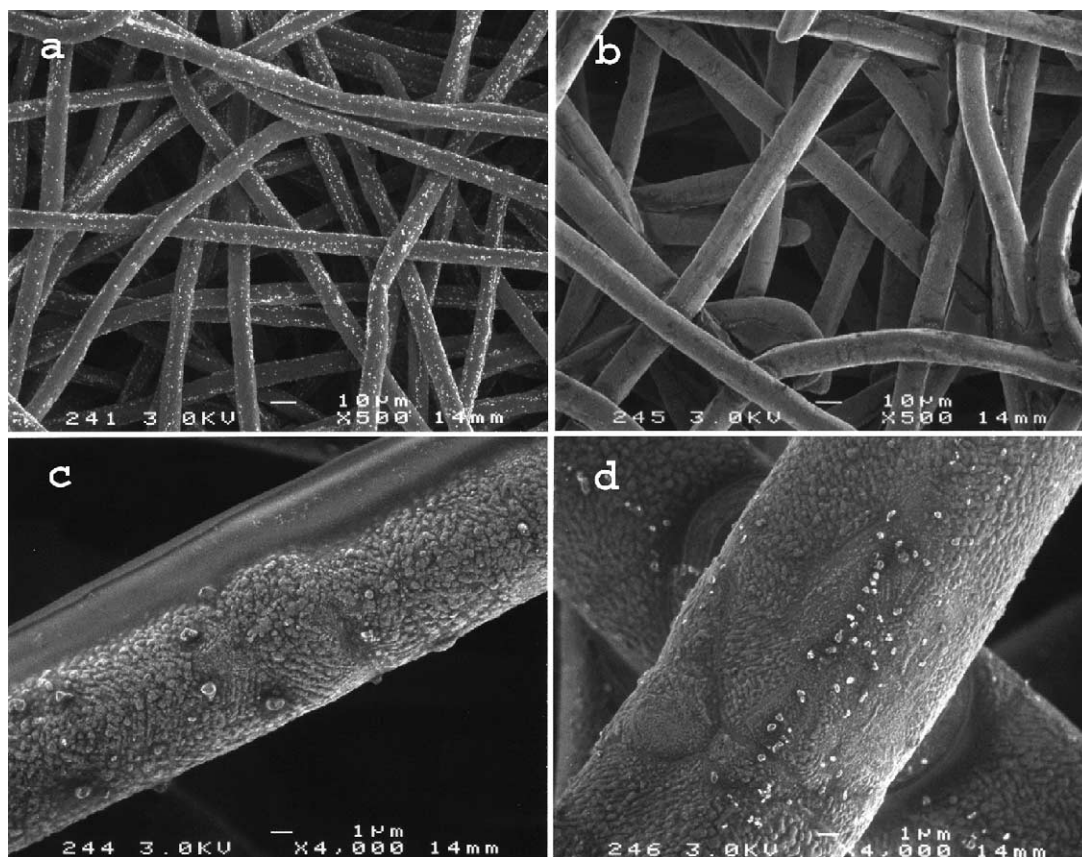
Fig. 2. SEM images of non-coated and coated sintered metal fibre filters (MFF): (a) initial MFF; (b, d) microporous SiO$_2$ coated MFF; (c) mesoporous SBA-15 coated MFF.

3. Results and discussion

3.1. Morphology of the catalysts

The SEM images of the non-coated and coated sintered metal fibres are presented in Fig. 2. As can be seen, thin homogeneous crack-free oxide films were formed on the metal fibre surface, and no peeling of the oxide films was observed during calcination (450–500 °C) and catalytic testing. The SEM investigations demonstrated that coated filters retained their open macrostructure. The thickness of the oxide films was estimated in the range of 0.5–0.8 μm.

Low-temperature N$_2$ adsorption–desorption measurements revealed that the SiO$_2$, Al$_2$O$_3$, and porous glass films were microporous with a pore diameter less than 2 nm (Table 2) and possessed the SSA of 250–350 m^2/g. For the SBA-15/MFF, the adsorption–desorption isotherms were of type IV with a H$_1$ hysteresis loop (Fig. 3) corresponding to well-ordered mesoporous structures [18,19]. The SBA-15 coating had a high specific surface area of ∼710 m^2/g (Table 2), a pore specific volume of 1.06 cm^3/g and narrow pore size distribution with an average pore diameter of ∼5.7 nm (Fig. 3). It is known that the supported SBA-15 films prepared by different methods have a highly oriented hexagonal structure with pore channels parallel to the support surface [16,17]. The SBA-15 mesoporous silicas show higher thermal stability compared to others mesoporous materials like MCM-41, MSU, HMS, etc. attributed to a large wall thickness (4–5 nm) [18]. The
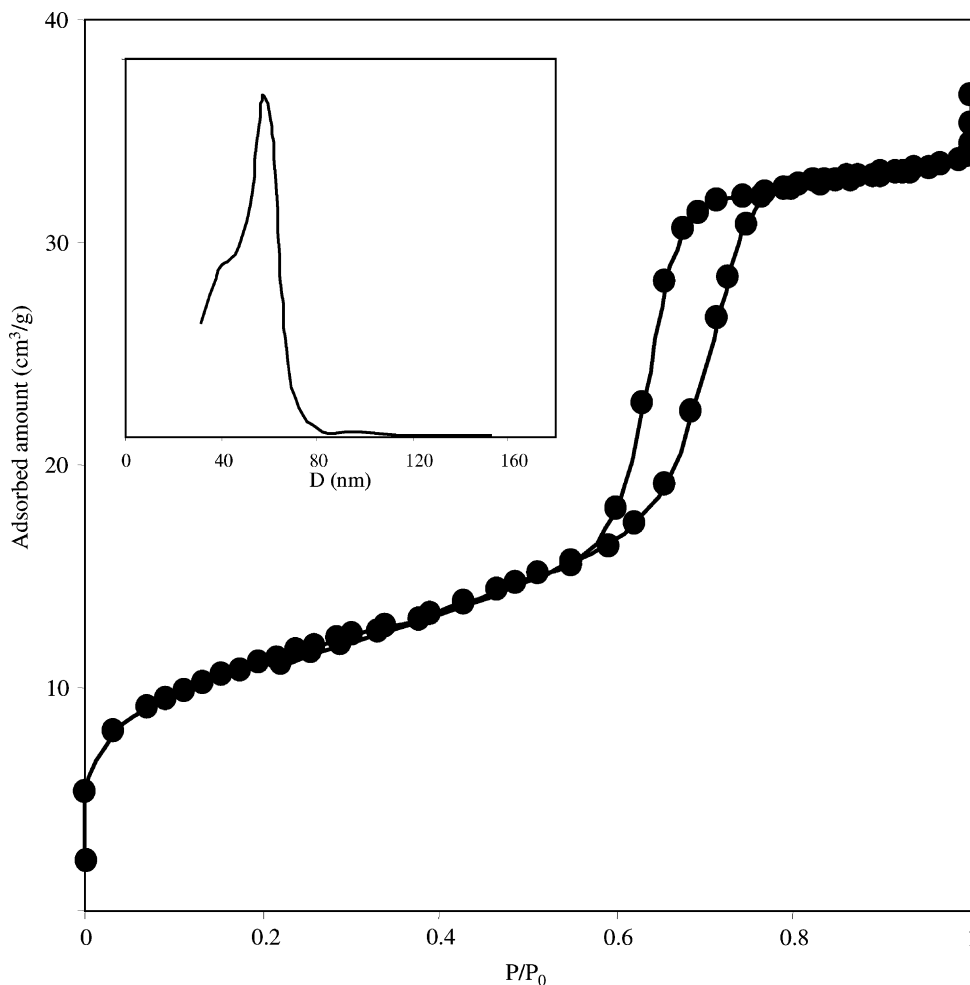
Fig. 3. N_2 adsorption–desorption isotherms of the SBA-15/MFF support. Inset: pore size distribution.

SBA-15 showed to be a suitable support for combustion catalysts [9].

Dispersion of Pd and Pt supported on the sintered MFF was found to be dependent on the oxide coating used (Table 2). The biggest Pd particles ($d > 70$ nm), detected on the non-coated metal fibres, were due to strong metal sintering during the catalyst preparation and hydrocarbon combustion. The average diameter of Pd particles on the microporous SiO_2 and Al_2O_3 films prepared by sol–gel (solvent evaporation) technique was of 30–50 nm. It is likely that Pd particles are mainly formed on the outer surface of the SiO_2 and Al_2O_3 films, not preventing metal sintering at elevated

temperatures. Besides, the collapse of oxide microporous structures at temperatures of 400–550 °C may lead to partial metal encapsulation resulting in a lower apparent dispersion.

The average Pd particle size in the MFF catalyst coated by mesoporous SBA-15 film measured after calcination and catalytic testing was found to be ∼1.7 nm and not to exceed the mesopore diameter (∼5.7 nm). The same behaviour was observed for Pt supported on the mesoporous SBA-15/MFF. Pt nanoparticles (∼2 nm) were found to be stable against agglomeration up to 500 °C. We have recently shown [9] that Pd particles supported on SBA-15 are formed

within mesopores and strongly attached to the pore walls. The maximum particle size is controlled by the pore diameter. The entrapped Pd nanoparticles are resistant against sintering at elevated temperatures.

The structure of the porous glass coating differs significantly from the silica gel porous structure. The structure of porous glass resembles a rigid sponge composed of almost pure SiO_2, whereas the porous structure of a silica gel is built of $(SiO_2)_n \cdot (H_2O)_m$ globules [14]. As a result, the porous glass has a higher mechanical and thermal resistance. It is stable up to $600\,^\circ C$ [13]. The average diameter of Pd particles supported on the porous glass film was found to be ~ 3.9 nm. This suggests that Pd particles are not only on the glass outer surface, but mostly are introduced inside the micropores. The walls of the porous glass separate Pd particles from each other leading to increased resistant against sintering and rendering catalyst with high Pd dispersion.

The introduction of Co-oxide in the mesoporous coating (1.4% Co_3O_4/SBA-15/MFF) seems to result in Co_3O_4 nanoclusters encapsulated in the pore channels as also reported in [20,21]. This process was manifested by the reduced SBA-15 specific pore volume from 1.20 to $0.51\,cm^3/g$ and average pore size from 6.0 to 3.9 nm (Tables 1 and 2). The SEM investigations of the 6.8% Co_3O_4/MFF catalyst revealed that on the non-coated metal fibre surface cobalt oxide was deposited as big agglomerates $(0.1–1.0\,\mu m)$.

3.2. Propane combustion

The temperature dependences of propane conversion over different catalysts are shown in Fig. 4. The temperatures of 50% conversion used for the comparison of catalytic activities are listed in Table 2. No catalyst deactivation in propane combustion was observed up to $450\,^\circ C$.

Among all studied catalysts, the 6.8% Co_3O_4/MFF and 1.4% Co_3O_4/SBA-15/MFF had the highest and lowest activity, respectively. As reported by different authors [6,22–24], cobalt oxide based catalysts generally are very active in total hydrocarbon oxidation. However, their activity depends on the cobalt oxidation state under the reaction conditions. In particular, catalytic performance of cobalt oxide is dependent on the propane/oxygen ratio [6,22]. The pre-reduced catalyst demonstrates higher activity and stability in a sto-
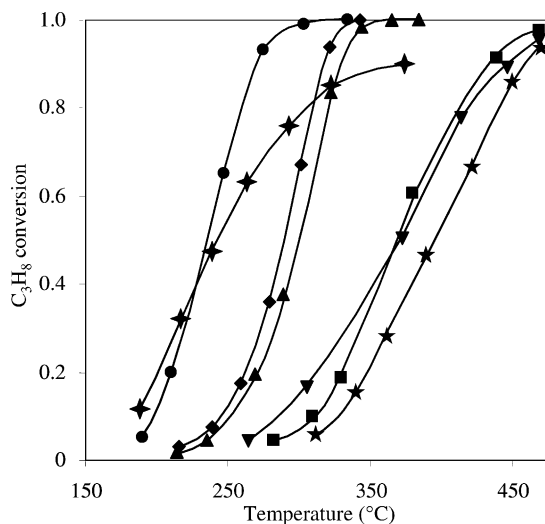

Fig. 4. Total oxidation of propane over MFF catalysts: (◆) 0.5% Pd/SBA-15/MFF; (▲) 0.5% Pd/PG/MFF; (■) 0.5% Pd/Al$_2$O$_3$/MFF; (★) 1.4% Co$_3$O$_4$/SBA-15/MFF; (●) 6.8% Co$_3$O$_4$/MFF; (✦) 0.5% Pt/SBA-15/MFF; (▼) 0.5% Pd/SiO$_2$/MFF.

ichiometric reactant mixture. In a mixture containing excess of oxygen, a strong deactivation was observed. The initial high catalytic activity could be recovered by reductive treatment of the catalysts. This behaviour was assigned to partial reduction of the Co oxide particles. Highly dispersed metallic Co species on the particle surface were responsible for the enhanced catalyst activity [6,22]. Oxidation of partially reduced active phase during propane combustion in excess of oxygen leads to catalyst deactivation. Under steady-state reaction conditions, the oxidation–reduction equilibrium on the surface of cobalt oxide particles controls the amount of active metallic Co species and hence the catalyst performance. It was found that mesoporous silica matrix strongly affects the cobalt oxide reduction: smaller particles in the narrow pores (2–5 nm) are much more difficult to reduce by hydrogen to the metallic state than big ones situated in the larger pores (>5 nm) [21]. So, in the case of the 1.4% Co_3O_4/SBA-15/MFF catalyst containing cobalt oxide mainly in the form of nanoclusters dispersed in the silica mesopores ($d \sim 6$ nm), the active phase is more difficult to reduce under the reaction conditions resulting in the low catalyst activity. On the contrary, in the 6.8% Co_3O_4/MFF catalyst, the readily reducible

big agglomerates of cobalt oxide (0.1–1.0 μm) seem
to be responsible for the higher catalyst activity.

It is generally agreed that the oxidised palladium
or PdO "skin" formed over supported Pd particles
is active in hydrocarbon combustion [25]. $Pd^{2+}O^{2-}$
ion pairs at the PdO surface activate the C–H bonds
via heterolytic mechanism, similar to that proposed
on metal oxide catalysts [26,27]. Pd and PdO are
in dynamic equilibrium depending on different pa-
rameters such as temperature, metal dispersion and
the reaction mixture composition. If we compare
different Pd catalysts tested in the present study,
the 0.5% Pd/SBA-15/MFF and 0.5% Pd/PG/MFF
demonstrated the higher activity in total propane ox-
idation (Fig. 4). The 0.5% Pd/SiO_2/MFF and 0.5%
Pd/Al_2O_3/MFF catalysts were found to be much
less active. Different metal dispersion (see Table 2)
can account for this behaviour. Moreover, the mi-
croporous SiO_2 and Al_2O_3 structures, prepared
through sol–gel technique, at elevated temperatures
may partially collapse resulting in metal nanoparti-
cles encapsulation and consequently lower catalytic
activity.

By contrast to Pd-based catalysts, it was proposed
that Pt activates the C–H bonds through a homolytic
mechanism via dissociative adsorption of hydrocar-
bon on surface metal sites. Oxygen species act as an
inhibitor for the reaction at full coverage [25,28]. As
we reported previously [3], the catalytic activity of Pt
(0.1–0.3 wt.%) supported on glass fibres modified by
different metal oxides (Al_2O_3, TiO_2) in propane oxi-
dation is much higher at temperatures <350 °C than
the activity of analogous Pd catalysts. The reaction
kinetics over Pt/glass fibres drastically differs from
the kinetics over Pd catalysts. The propane conversion
over the former catalysts was observed to increase
slower with temperature, indicating lower apparent
activation energy. The observed reaction order over
Pt catalysts was found to be negative with respect
to O_2 due to reaction inhibition by oxygen [3,28].
In the present study, the 0.5% Pt/SBA-15/MFF cat-
alyst revealed to be also more active than the 0.5%
Pd/SBA-15/MFF at temperatures <300 °C in spite
of the lower molar content of active metal (Fig. 4).
At higher temperatures, the reverse situation was ob-
served indicating different apparent activation energies
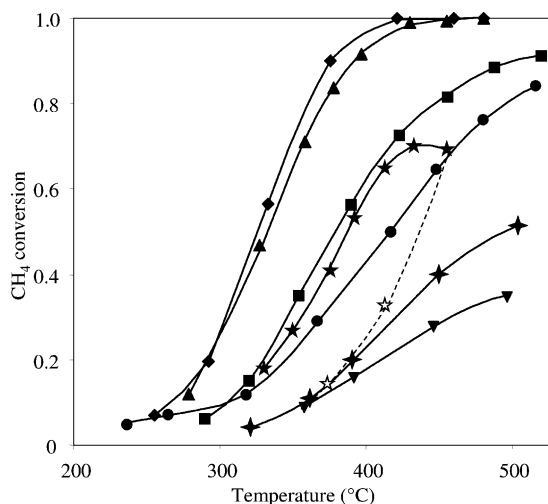for the propane total oxidation over these two types of
catalysts.

Fig. 5. Total oxidation of methane over MFF catalysts: (◆) 0.5%
Pd/SBA-15/MFF; (▲) 0.5% Pd/PG/MFF; (■) 0.5% Pd/Al_2O_3/
MFF; (★) 0.5% Pd/MFF; (●) 6.8% Co_3O_4/MFF; (✦) 0.5%
Pt/SBA-15/MFF; (▼) 0.5% Pd/SiO_2/MFF. Deactivation is shown
only for the 6.8% Co_3O_4/MFF catalyst: solid line: temperature
increases; dotted line: temperature decreases.

3.3. Methane combustion

As compared to the propane combustion, the tem-
peratures of 50% methane conversion over studied
catalysts were found to be considerably higher. Deac-
tivation indicating metal sintering and/or collapse of
oxide coating structures was observed for some cat-
alysts (Table 2). The 0.5% Pd/MFF catalyst without
any coating presented the most pronounced deacti-
vation (Fig. 5). At the same time, it is worth to note
that this catalyst shows the higher activity as com-
pared to the 0.5% Pd/SiO_2/MFF, which has higher
Pd dispersion. It clearly demonstrates the influence
of the support composition on the catalytic activity
of supported palladium, being in line with the data
reported [25] that the transition metal oxides signif-
icantly improve the Pd catalytic performance. The
0.5% Pd/SBA-15/MFF and 0.5% Pd/PG/MFF charac-
terised by the high metal dispersions (66.0 and 29.8%,
respectively) were the most active and stable in
methane combustion. Metal nanoparticles entrapped
in the confined space of SBA-15 and PG structures
are resistant against agglomeration [9]. At the same
time, the catalysts demonstrated almost the same tem-
perature of 50% methane conversion (Table 2). This

result confirms that the presence of both PdO and metallic Pd in the active phase defines the Pd catalyst activity [25]. In the 0.5% Pd/SBA-15/MFF highly dispersed palladium seems to be completely oxidised under oxygen-rich reaction conditions. By contrast, the 0.5% Pd/PG/MFF catalyst characterised by more than two times lower metal dispersion contains a PdO skin on a Pd metal core resulting in the higher activity per a surface Pd atom.

In contrast to propane combustion, 0.5% Pt/SBA-15/MFF catalysts were observed to be much less active in methane total oxidation, being in agreement with the results reported for Pt catalysts by different authors [25,28]. It is likely that under conditions of high temperatures and oxygen-rich atmosphere, the Pt surface is blocked by oxygen species acting as an inhibitor. The formation of PtO_2 was reported above 300 °C in the case of 100% dispersed Pt particles [29]. The high temperature transformation of active metallic Co species to Co_3O_4 seems to be a reason for the relatively low activity of the 6.8% Co_3O_4/MFF in methane total oxidation (Table 2, Fig. 5).

3.4. Structured multi-layered catalytic beds in propane combustion

The catalytic elements made from sintered metal fibre panels allow designing of structured catalytic beds consisting of different active phases (gradient catalytic bed). When catalytic combustion is carried out in an adiabatic reactor, such gradient arrangement should allow taking advantage of the catalytic layers with a lower light-on temperature to ignite the reaction. The following elements containing a catalyst more active at higher temperatures should benefit from the heated reaction mixture. To show fruitfulness of such approach the C_3H_8 combustion was performed over a structured multi-layered catalytic bed composed from the 0.5% Pt/SBA-15/MFF and 0.5% Pd/SBA-15/MFF catalysts. As described above, the 0.5% Pt/SBA-15/MFF has a lowest start-up temperature, and the 0.5% Pd/SBA-15/MFF catalyst is more active at higher temperatures. The gradient catalytic bed was formed from three catalytic filters of different chemical compositions. The ratio of Pt- and Pd-containing disks was varied and they were assembled in different orders.
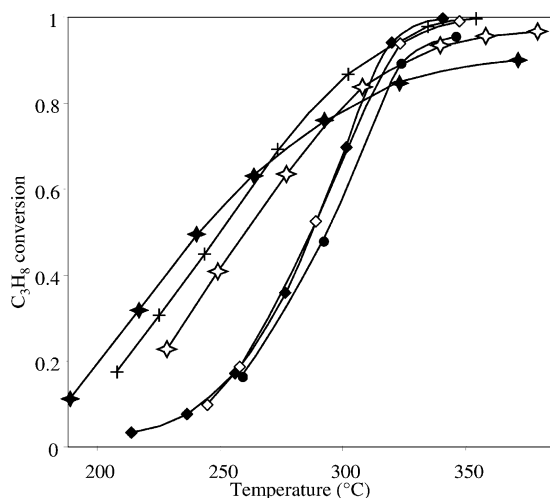

Fig. 6. Total oxidation of propane over multi-layered gradient catalytic beds: (◆) 3 × (0.5% Pd/SBA-15/MFF); (✚) 3 × (0.5% Pt/SBA-15/MFF); (◇) 2 × (0.5% Pd/SBA-15/MFF) and 1 × (0.5% Pt/SBA-15/MFF); (●) 1 × (0.5% Pd/SBA-15/MFF) and 2 × (0.5% Pt/SBA-15/MFF); (✦) 1 × (0.5% Pt/SBA-15/MFF) and 2 × (0.5% Pd/SBA-15/MFF); (+) 2 × (0.5% Pt/SBA-15/MFF) and 1 × (0.5% Pd/SBA-15/MFF).

The results of the propane combustion over structured multi-layered catalytic beds are presented in Fig. 6. The order of filters in respect to the gas flow direction is noted in the catalyst designations. At lower temperatures and lower propane conversions, three 0.5% Pt/SBA-15/MFF filters are more active than three 0.5% Pd/SBA-15/MFF filters. At higher temperatures and higher conversions, the reverse situation was observed. As could be expected, the multi-layered catalytic bed with the 0.5% Pd/SBA-15/MFF filters placed upstream in respect to the 0.5% Pt/SBA-15/MFF filters always demonstrated lower overall conversion if compared to the uniform 0.5% Pd/SBA-15/MFF catalytic bed. During the passage of the gas mixture through the Pd containing filters positioned first in the reactor, the adiabatic heat released increases the temperature at which the Pt containing filters could not provide high propane conversion. At the contrary, the catalytic beds containing the 0.5% Pd/SBA-15/MFF filters positioned downstream in respect to the 0.5% Pt/SBA-15/MFF filters showed higher overall conversion in the whole temperature range. Moreover, in the vicinity of 300 °C these catalytic beds are more active than both

non-gradient beds. This synergistic effect is due to the different kinetics of propane combustion over Pd and Pt catalysts. Therefore, the adiabatic heating of the gas mixture during the passage through the Pt catalytic filter positioned first provides the reaction ignition and favours the performance of the 0.5% Pd/SBA-15/MFF catalysts.

4. Conclusions

- Novel structured combustion catalysts based on sintered metal fibre filters (MFF) were developed. The materials have an increased SSA obtained *via* coating of MFF by different crack-free porous oxide films like SiO_2, Al_2O_3, porous glass, and mesoporous SBA-15 silica.
- Catalytically active phases (Pd, Pt, and Co_3O_4) were deposited on the coated MFF supports and the catalysts were tested during methane and propane combustion. The most active for propane total oxidation was Co_3O_4 supported on MFF without any coating (6.8% Co_3O_4/MFF). Pd supported on the MFF coated by mesoporous SBA-15 film (0.5% Pd/SBA-15/MFF) demonstrated the best performance in methane total oxidation.
- The particle size and catalytic properties of noble metals (Pd, Pt) supported on the MFF composites were observed to depend on the oxide coating. The catalysts with the mesoporous SBA-15 and porous glass films have the highest dispersion of the noble metals (1.7–3.9 nm) and are stable against agglomeration up to 500 °C. On the contrary, the Pd catalysts based on MFF coated by microporous SiO_2 and Al_2O_3 films prepared by sol–gel technique, suffered from metal sintering and collapse of the support microporous structure, which occurred at high temperatures.
- The developed catalytic filters are suitable materials for assembling different multiple layers to obtain structured catalytic beds with the composition/concentration gradient of active component in the axial direction. The enhanced overall catalytic performance was observed in adiabatic catalytic reactor during propane combustion due to a synergy of the 0.5% Pd/SBA-15/MFF and the 0.5% Pt/SBA-15/MFF catalytic layers assembled in the appropriate order forming gradient catalytic bed.

References

[1] A. Cybulski, J. Moulijn (Eds.), Sructured Catalysts and Reactors, Marcel Dekker, New York, 1998.
[2] L. Kiwi-Minsker, I. Yuranov, B. Siebenhaar, A. Renken, Catal. Today 54 (1999) 39.
[3] L. Kiwi-Minsker, I. Yuranov, E. Slavinskaia, V. Zaikovskii, A. Renken, Catal. Today 59 (2000) 61.
[4] W. Gürtler, J. Ackermann, G. Emig, Chem. Ing. Technol. 68 (1996) 1438.
[5] W. Gürtler, Patent No. 19611395C1, Germany (1997).
[6] I. Yuranov, N. Dunand, L. Kiwi-Minsker, A. Renken, Appl. Catal. B: Environ. 36 (2002) 183.
[7] R. De Bruyne, Multipass Test Performance of Metal Fibre Filter Media, World Filtration Congress III, Downingtown, 1982, p. 400.
[8] D.R. Cahela, B.J. Tatarchuk, Catal. Today 69 (2001) 33.
[9] I. Yuranov, P. Moeckli, E. Suvorova, P. Buffat, L. Kiwi-Minsker, A. Renken, J. Mol. Catal. A: Chem. (2003), in press.
[10] M. Ogawa, K. Kuroda, J. Mori, Langmuir 18 (2002) 744.
[11] M. Ogawa, J. Am. Chem. Soc. 116 (1994) 7941.
[12] M.B. Volf, Technical Glasses. Pitman, London, 1961.
[13] H. Wang, G.R. Gavalas, J. Membr. Sci. 176 (2000) 75.
[14] A.L. Dawidowicz, in: A. Dabrowski, V.A. Tertykh (Eds.), Studies in Surface Science and Catalysis, vol. 99, Elsevier, Amsterdam, 1996, p. 31.
[15] K. Haas-Santo, M. Fichtner, K. Schubert, Appl. Catal. A: Gen. 220 (2001) 79.
[16] T. Yamada, K. Asai, A. Endo, H.S. Zhou, I. Honma, J. Mater. Sci. Lett. 19 (2000) 2167.
[17] D. Zhao, P. Yang, N. Melosh, J. Feng, B.F. Chmelka, G.D. Stucky, Adv. Mater. 10 (1998) 1380.
[18] D. Zhao, Q. Huo, J. Feng, B.F. Chmelka, G.D. Stucky, J. Am. Chem. Soc. 120 (1998) 6024.
[19] D. Zhao, J. Feng, Q. Huo, N. Melosh, G.H. Fredrickson, B.F. Chmelka, G.D. Stucky, Science 279 (1998) 548.
[20] Y. Wang, M. Noguchi, Y. Takahashi, Y. Ohtsuka, Catal. Today 68 (2001) 3.
[21] A.Y. Khodakov, A. Griboval-Constant, R. Bechara, F. Villain, J. Phys. Chem. B 105 (2001) 9805.
[22] A. Törncrona, M. Skoglundh, P. Thormählen, E. Fridell, E. Jobson, Appl. Catal. B: Environ. 14 (1997) 131.

[23] A.K. Neyestanaki, L.-E. Lindrofs, Combust. Sci. Technol. 110–111 (1995) 303.

[24] M.F.M. Zwinkels, S.G. Järås, P.G. Menon, Catal. Rev. Sci. Eng. 35 (1993) 319.

[25] P. Gélin, M. Primet, Appl. Catal. B: Environ. 39 (2002) 1.

[26] V.R. Choudhary, V.H. Rane, J. Catal. 130 (1991) 411.

[27] R. Burch, D.J. Crittle, M.J. Hayes, Catal. Today 47 (1999) 229.

[28] T.V. Choudhary, S. Banerjee, V.R. Choudhary, Appl. Catal. A: Gen. 234 (2002) 1.

[29] R.W. McCabe, C. Wong, H.S. Woo, J. Catal. 114 (1988) 354.